INTERNATIONAL JOURNAL OF OPTIMIZATION IN CIVIL ENGINEERING
Int. J. Optim. Civil Eng., 2019; 9(1):39-63

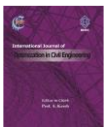

MINIMUM WEIGHT AND DRIFT DESIGN OF STEEL MOMENT FRAMES SUBJECTED TO BLAST

N. Khaledy[1], A.R. Habibi[2*, †] and P. Memarzadeh[1]
[1]*Department of Civil Engineering, Najafabad branch, Islamic Azad University, Najafabad, Iran*
[2]*Department of Civil Engineering, Shahed University, Tehran, Iran*

ABSTRACT

Design of blast resistant structures is an important subject in structural engineering, attracting the attention of governments, researchers, and engineers. Thus, given the benefits of optimization in engineering, development and assessment of optimization methods for optimum design of structures against blast is of great importance. In this research, multi-objective optimization of steel moment frames subjected to blast is investigated. The considered objectives are minimization of the structural weight and minimization of the maximum inter-story drifts. The minimization of weight is related to obtain low cost designs and the minimization of inter-story drifts is related to obtain higher performance designs. By proposing a design methodology, a framework is developed for solving numerical problems. The developed framework is constructed by combining explicit finite element analysis of the structure and the NSGA-II optimization algorithm. The applicability and efficiency of the proposed method is shown through two numerical examples.

Keywords: blast; nonlinear design; multi-objective; optimization; NSGA-II.

Received: 20 February 2018; Accepted: 10 May 2018

1. INTRODUCTION

In today's world, terrorist attacks and wars are phenomena which threaten human security all over the world. Meanwhile, structures play an important role in either increasing or decreasing damages or losses. Also as it's true for other types of loads, if a structure is to be designed to have an appropriate performance against potential events and their subsequent loadings, it will bring psychological comfort for residents and the whole society even though they never occur. Thus, it is very important to conduct more studies on the behavior of

[*]Corresponding author: Department of Civil Engineering, *Shahed University, Tehran, Iran*
ar.habibi@shahed.ac.ir (A.R. Habibi)

structures against blast and the resistant design against this type of loading, particularly under current conditions and events in the world.

Preliminary researches on blast loading, behavior and resistant design of structures against blast date back to the years of World War II [1-3]. But most studies in this field have been conducted in the about past 15 years. Some of the important researches in recent years carried out on steel structures are as follows:

Hadianfard et al. [4] studied the effect of steel columns cross-sectional properties on their behaviors when subjected to blast. Using ANSYS software, the researchers analyzed some steel columns with different shapes of the cross-section and different boundary conditions, subjected to blast loading. The researchers concluded that shape and elastic-plastic properties of sections and also boundary conditions of columns play important roles on the response of steel columns subjected to blast.

Nassr et al. [5] modeled steel beam and beam-columns against blast load using single and multi-degree of freedom models. First, the researchers conducted an experimental study to evaluate responses of some wide flange beams subjected to blast. Then, the authors compared the results of the SDOF and MDOF models with the experimental tests. Based on the results, it was shown that both proposed single and multi-degree of freedom models could predict the history of responses with a good accuracy. Also, the researchers concluded that the use of a constant strain rate to calculate Dynamic Increase Factor (DIF) would lead to a conservative design.

Using passive unidirectional dampers, Monir [6] conducted a research on the resistant steel structures against blast. The researcher presented a new uni-directional passive damper which shows different performance against compression and tension. The author concluded that by using this type of dampers in a ductile frame, a resistant structure would be obtained which it could absorb most of the blast energy.

Nassr et al. [7] evaluated the resistance and stability of steel beam-columns subjected to blast loading. The researchers used a one-degree of freedom model for studying the effects of axial load on the strength and stability of columns subjected to blast. The model was validated by comparing the results with experimental results and also finite element analysis. Comparing the results of the one-degree of freedom model and results from UFC 3-340-02 code, showed that regardless of axial load to the Euler critical load ratio, the UFC method overestimates the column's capacity for ductility coefficients greater than one.

Coefield and Adeli [8] examined the performance of earthquake-resistant bracing systems against blast. The researchers studied three structural systems including a Moments Resistant Frame (MRF), a Centrally Braced Frame (CBF) and an Eccentrically Bracing Frame (EBF), designed for the earthquake. The results showed that the CBF system had a better resistance level in the blast scenarios considered in the study.

Elsenadedy et al. [9] studied the potential of progressive collapse in steel structures subjected to blast attacks. The researchers analyzed a conventional multi-story steel frame against blast to evaluate its vulnerability in accidental or terroristic blast scenarios. Based on the results of finite element analysis, the authors proposed strategies for reducing or controlling potential progressive collapse in steel structures.

Lee and Shin [10] studied equivalent single-degree of freedom analysis for blast-resistant design. The researchers extended the available SDOF elastic-plastic design charts to be used for near field explosions. The results are verified using the UFC-3-340-02 and LS-DYNA

finite element code. Since the available charts in the UFC are provided for far-field detonations, the authors suggested using the proposed charts in the near-field cases.

On the other hand, the optimum design of structures given numerous advantages such as cost and time savings is of great importance in structural engineering. Due to advances in the fields of computers and processors, optimization science has undergone a great progress. It is always updated along with new situations and needs of the day. Some of the recent researches have been carried out on the multi-objective optimization of steel frames are as follows:

Kaveh et al. [11] proposed a method for performance-based seismic multi-objective optimization of large steel structures. The considered objective functions were the initial and the life-cycle cost of large structures. Pushover analysis was used as the structural analysis method and the NSGA-II method was used as the multi-objective optimization algorithm. The researchers concluded that the proposed method is effective for solving the studied problem.

Based on the history of nonlinear responses, Gong et al. [12] presented a method for optimum design of steel frames under seismic loads. Minimization of weight, minimization of input earthquake energy and maximization of energy absorption, were considered as the three objective functions. Also, story drifts and plastic hinge rotation in members were considered as design constraints. A three-story building was studied as the numerical example. The researchers concluded that the proposed method is an efficient method for designing steel frames under seismic loadings.

Kaveh et al. [13] studied multi-objective performance-based design of steel frames under seismic loading. Minimization of the structural weight and the seismic damage of steel moment frames were considered as the optimization objectives. A method was proposed for solving the studied problem using NSGA-II optimization algorithm. The researchers showed the efficiency of the method by considering some numerical examples.

Gholizadeh and Baghchevan [14] studied the seismic multi-objective optimization of steel frames using a chaotic multi-objective firefly algorithm (CMOFA). The structural weight and the maximum inter-story drifts were considered as the objective functions. By reviewing some numerical examples, the researchers showed the superiority of the CMOFA method in comparison with some other multi-objective algorithms.

Babaei and Sanaei [15] studied the multi-objective optimum design of braced steel frames using a hybrid optimization algorithm. The optimization algorithms consisted of the Genetic and the Ant Colony algorithms. The objective functions were considered as the structural weight and the maximum displacement of the structure. By considering weight coefficients for the two objective functions in the studied examples a trade-off was obtained between two objective functions. The researchers concluded that the proposed method is capable of finding optimal topologies and sections for the elements.

Barraza et al [16] studied the multi-objective optimum design of steel structures under seismic loading using NSGA-II and PSO algorithms. The structural weight and the maximum story drifts were considered as the objective functions. Member sections were chosen from a list of 256 AISC W sections. The researchers concluded that both the Non-dominated Sorting Genetic Algorithm (NSGA II) and the Particle Swarm Optimization (PSO) algorithm are capable to reduce the structural weight and improve the structural performance. Also, the authors concluded that the PSO algorithm had better results in the

studied multi-objective optimization problem.

Rezazadeh et al. [17] studied the multi-objective optimization of steel frames with Buckling Resistant Braces (BRB) using nonlinear response history analysis. Minimization of the structural weight and input seismic energy were considered as the optimization objectives. The main constraints were considered as the story drifts, plastic rotation in beams and columns, and the plastic displacement of the buckling resistant braces. The multi-objective charged system search (MoCSS) method was used as the optimization algorithm. The researchers concluded that the studied method is effective and gives the optimal solutions as the Pareto optimal solutions.

The literature review reveals that in the field of multi-objective optimum design of framed structures, most of works have been done on the optimization of structures under earthquake seismic loadings. Since there are essential differences in loading, behavior, analysis and design of structures under earthquake and blast, there is a gap on the field to be filled by more researches on the multi-objective optimization of structures against blast. The main purpose of the present study is to develop and evaluate a methodology for the multi-objective optimum design of steel moment frames under blast loading, to obtain low cost and high performance designs.

2. BLAST LOADING

Blast load is a time-history loading which occurs in a very short period. Generally, its time-history diagram is as shown in Fig. 1.

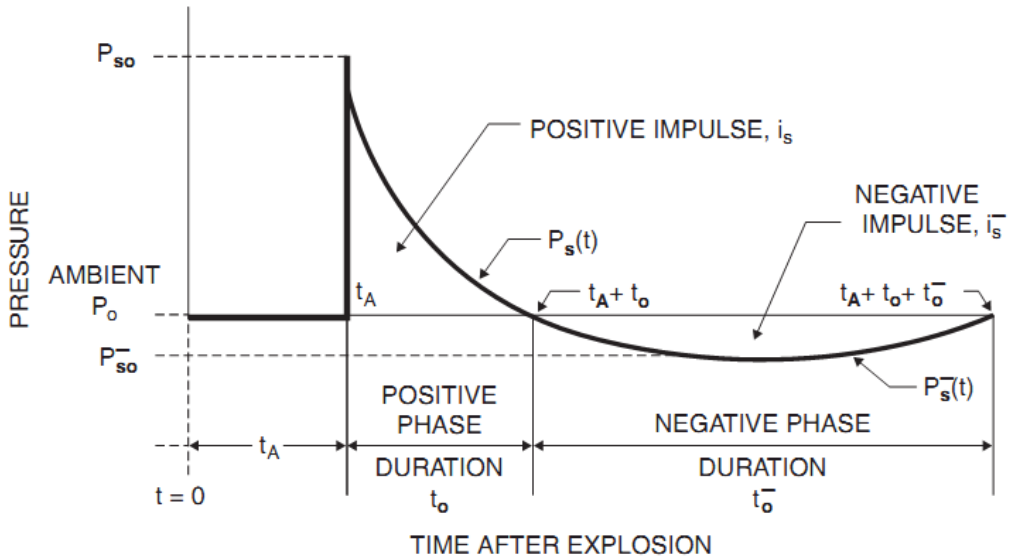

Figure 1. General time-history diagram for blast loading [18]

When an explosion occurs on the earth surface or in front of a structure where blast waves can be reflected, this reflection amplifies the blast loading, and in this case, the

effective blast pressure would be P_r. Explosions which occur on the surface of the earth are called Surface bursts (blasts), and explosions which occur in the air are called Air bursts (blasts). The most important parameters associated with blast loading, include maximum effective pressure (P_r or P_o), impulse (the area under time-pressure diagram), and the duration of the positive phase, respectively. It should also be noted that all of the main parameters related to the blast loading are functions of type and mass of the explosive, the distance between explosion source and the structure (standoff), and the type of blast (Surface or Air). Calculation of these parameters can be made by some empirical equations or graphs that are presented in references such as UFC 3-340-02 [18], Blast Effects on Buildings [19] and ASCE 59-11 [20].

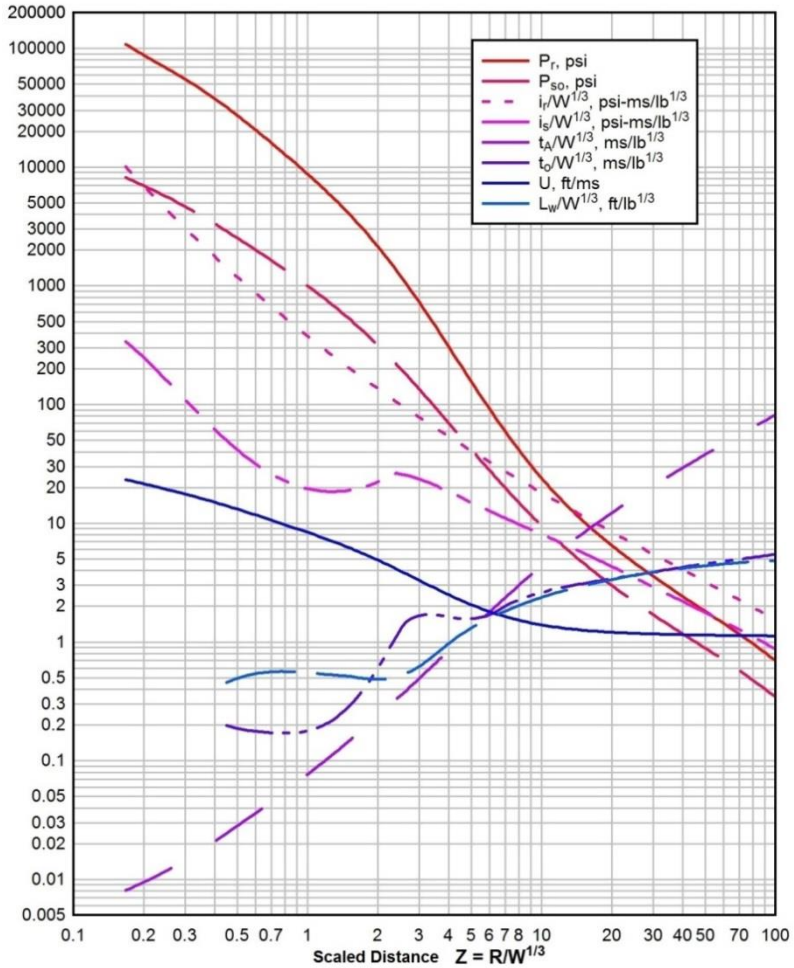

Figure 2. A diagram for calculating blast loading parameters [18]

In this graph Z is the scaled distance of blast:

$$Z = \frac{R}{W^{1/3}} \qquad \text{Eq.} \tag{1}$$

where R is the standoff distance and W is the mass of equivalent TNT of explosive.

In blast events, the effective pressure decreases as a nonlinear function by moving away from the source of the explosion, so that the local effects should be considered in near-range explosions. Based on ASCE 59-11 [20] if the scaled distance Z be greater than 3 $ft/lb^{1/3}$ (1.2 $m/kg^{1/3}$) the explosion is classified as far-range, and the loading can be considered as a uniform distributed time-history load acting on the structure. In the current study, blast events are assumed to be in the far range. It should be noted that when a blast wave interact with a structure, the blast overpressure will act on the front side, roof, and the rear side of the structure, but the arrival time of blast for each side of the structure is different. Also, because of the reflection effects, the front side of a given structure experiences much higher blast pressure than its other sides. Therefore in some researches only the front side loading is considered [6], [21-23]. In the presented study it is assumed that the blast load only acts on the front side of a given structure and blast loading on the other sides are neglected.

The quantity and blast characteristics a given structure is designed for, depends on various factors such as the history of terrorist attacks, the importance of the building, ease of access to the building or terroristic target, the number of occupants of the building, distance from the structure and ease of access to the threatening materials [24]. Based on these factors, a simplified method is proposed in [24] for terroristic threats risk assessment. Also, there are some diagrams which can be used to estimate the potential blast capacity of some blast threats. Based on these diagrams, for example, a sedan car has a capacity of carrying a mass between 100-500 lbs. (45-226 kg) of TNT.

3. NONLINEAR DYNAMIC ANALYSIS

In this research, the structural analysis has been performed by finite element analysis using Abaqus FE analysis software [25]. In the finite element analysis, the nonlinear dynamic analysis is performed by direct integration methods. Direct integration methods can be performed by two different procedures: Implicit approach and explicit approach. In the "implicit" approach, it is required that in every step the structural stiffness matrix be inverted and nonlinear equations be solved. Thus, when the degrees of freedom are high, this method will be computationally expensive as it is required to calculate the inverse of the stiffness matrix and solve the nonlinear equations. In the "explicit" approach, velocity and displacement are calculated based on the known values at the beginning of each time step. Therefore, calculating the inverse of the stiffness matrix is not required. In other words, compared to the implicit method, this method requires less computational effort at each time step. However, the "implicit" method is numerically stable, while in "explicit" approach, time steps should be considered small enough to ensure the stability of the method. Thus, in dynamic problems that occur in a short time such as impact and explosion problems, the explicit method is better and requires less computational effort. Because of the mentioned computational advantages, the explicit method is used in this research.

One of the most popular explicit methods is the central difference method. In this method velocity and acceleration are written as follows [26]:

$$\dot{u}^{t+\Delta t} = \frac{u^{t+\Delta t} - u^{t-\Delta t}}{2\Delta t} \tag{2}$$

$$\ddot{u}^{t+\Delta t} = \frac{u^{t+\Delta t} - 2u^{t} + u^{t-\Delta t}}{\Delta t^2} \tag{3}$$

where $u, \dot{u}$, and $\ddot{u}$ are the displacement, velocity, and acceleration vectors, respectively. Also, Δt is the time step. Also, the equation of motion can be written as follows:

$$M\ddot{u}^{t+\Delta t} = f_{ext}^{t+\Delta t} - f_{int}^{t+\Delta t} \tag{4}$$

where, M is the global mass matrix, and f_{ext} and f_{int} are the external and internal forces vectors, respectively. By substituting Eq(3) in Eq(4) we have:

$$\frac{1}{\Delta t^2} M u^{t+\Delta t} = f_{ext}^{t+\Delta t} - f_{int}^{t+\Delta t} + \frac{1}{\Delta t^2} M(2u^{t} - u^{t-\Delta t}) \tag{5}$$

This equation can be solved for displacement in $t + \Delta t$:

$$u^{t+\Delta t} = \Delta t^2 M^{-1}\left(f_{ext}^{t+\Delta t} - f_{int}^{t+\Delta t}\right) + 2u^{t} - u^{t-\Delta t} \tag{6}$$

Then the displacement increment can be calculated as $\Delta u = u^{t+\Delta t} - u^{t}$, and the strain increment $\Delta\epsilon$ will be obtained based on the Kinematic relation. Also, the stress increment $\Delta\sigma$ can be obtained using the constitutive equations. The stress is updated using the following equation:

$$\sigma^{t+\Delta t} = \sigma^{t} + \Delta\sigma \tag{7}$$

And the internal forces vector can be derived as follows:

$$f_{int} = \sum_{e=1}^{n_e} Z_e^T \int_{V_e} B_T \sigma dV \tag{8}$$

where n_e is the number of elements, Z_e is the incidence or location matrix which relates the local and global coordinates of an element, and B is a matrix that relates the strains within an element with the nodal displacements. The above integration can be solved using numerical techniques like Gaussian or Simpson numerical integration techniques. Since in Eq(6) the displacement in $t + \Delta t$ is calculated based on the displacement in t and $t - \Delta t$, thus the displacement values in the two previous steps are required. This makes an initialization problem for t=0. To overcome this issue, the Eq(6) for t=0 is written as follows:

$$u^{-\Delta t} = u^{0} - \Delta t\dot{u}^{0} + \frac{1}{2}\Delta t^2 M^{-1}(f_{ext}^{0} - f_{int}^{0}) \tag{9}$$

where, u^0 and $\dot{u}^0$ are the initial displacement and the initial velocity vectors.

In the present study, the frame structures are modeled using B21 Timoshenko beam element [25]. Also, material nonlinearity is considered as elasto-plastic steel with iso-parametric hardening. Also, geometrical nonlinearity is considered in the analysis. Elements sizes (mesh size) are chosen by 1/10 of member's length. Also, strain rate effects are considered in the analysis according to UFC 3-340-02 [18] as shown in Fig. 3. To ensure the accuracy of the nonlinear finite element model and analysis, another available study is modeled based on the present research modeling assumptions. Nassr et al. [29] experimentally and analytically studied the response of some beam and beam-columns against blast. Here, two beams and two beam-columns which had been studied by Nassr et al. are modeled. In the modeled samples, each member length is 2413 mm and section profiles are W150X24. Also, yield stress of the steel material is 470 MPa as reported by Nassr et al. The experimental test setup is shown in Fig. 4. Also, a schematic drawing of the location of the charge and the samples is shown in Fig. 5. Summary of the modeled tests in the present study is shown in Table 1. Complete details of the experimental tests are described by Nassr et al. [29].

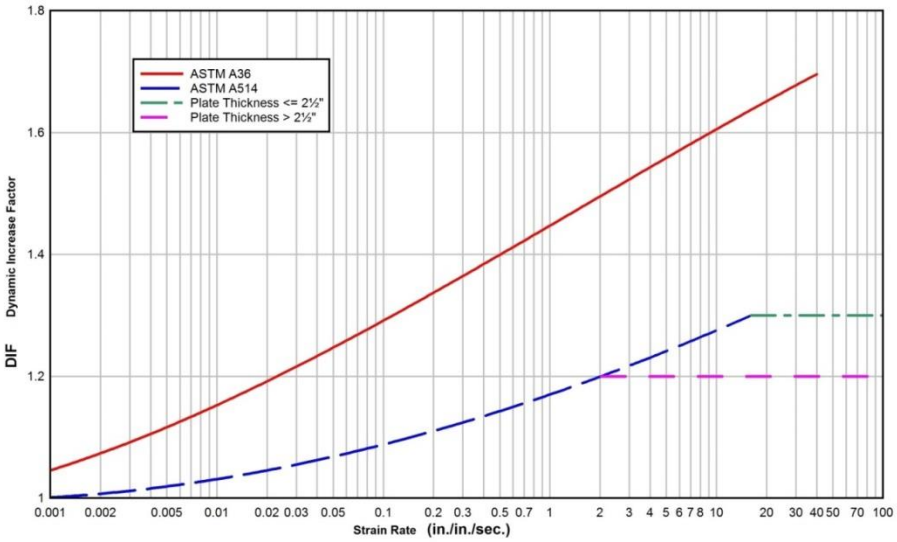

Figure 3. Strain Rate Effect (SRE) on Dynamic Increase Factor (DIF) [18]

Figure 4. The Experimental test setup [29]

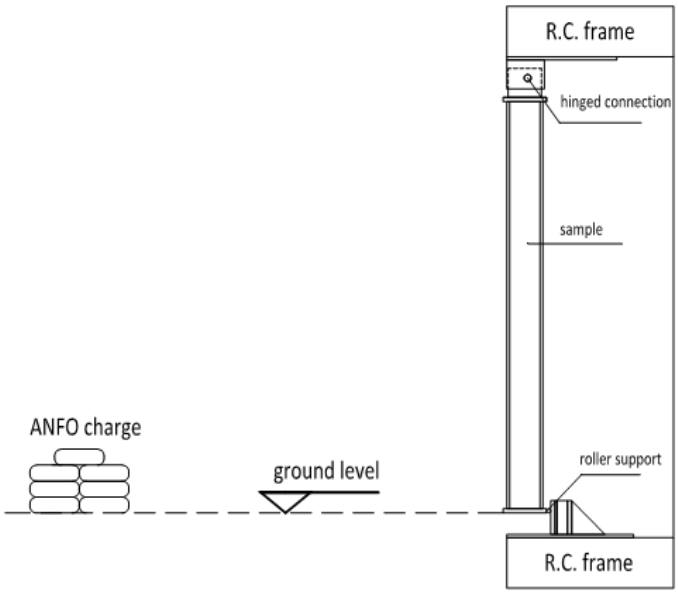

Figure 5. Schematic drawing of the charge and the samples location [29]

Table 1: Properties of the experiments selected for FE model validation

Sample Name	Bending Axis	Axial Load *(kN)*	Standoff *(m)*	Charge mass *ANFO (kg)*
B1	*x-x*	0	10.3	50
B2	*x-x*	0	9	150
C1	*y-y*	270	10.3	100
C2	*x-x*	270	9	150

In Figs. 6 to 9, history of mid-span deflection of modeled samples in the current study and the results reported by Nassr et al. are compared. As it is obvious, the used finite element model properly predicted the history of mid-span deflection of the members. In Figs. 6-9, differences between the maximum mid-span deflection in the current study and the experimental study of Nassr et al. [29] are 1.4%, 2.8 %, 0 and 3.1 % respectively. Also in these Figures, it is evident that the history of responses in the current study and the multi-degree of freedom model used by Nassr et al. have a high compatibility with each other. In both studies, beam elements are used. In the current study, each member is divided into 10 elements, and the Timoshenko beam elements are used. Nassr et al. had used Bernoulli beam elements, and each member was divided into 24 elements. It should be noted that in the process of verification it was observed that the sensitivity of responses was high to changes in the maximum blast pressure and the blast duration. Therefore, it seems that the very small differences in graphs, is due to the very small differences in the blast loading in the experimental test and the numerical model. In the current study, the blast load applied to the members by a uniform distributed time-history load, which in the experiments, based on the pressures measured by gauges, the pressure distribution had not been completely uniform over the member's length. In addition, in real conditions, due to shape and type of obstacles in the field, and the effect of reflection of blast waves, the actual diagram of blast loading

may not be exactly as the diagrams obtained by the equations and curves presented in manuals and design codes, which probably are derived in some specific and simplified conditions. It should be emphasized that the horizontal axes of the verification diagrams are in millisecond, and therefore differences between the compared graphs are very small.

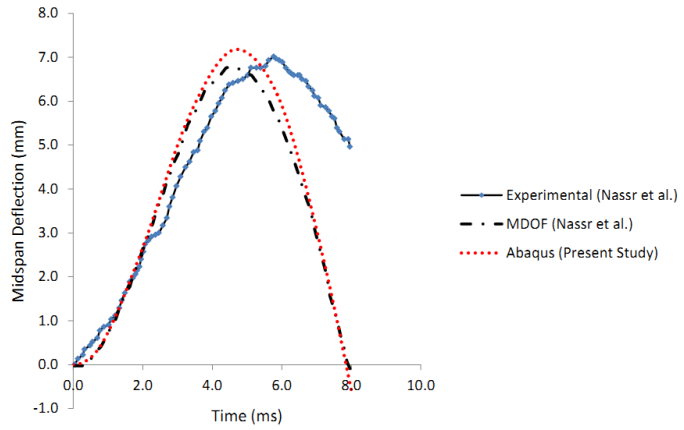

Figure 6. Mid-span deflection of B1 beam

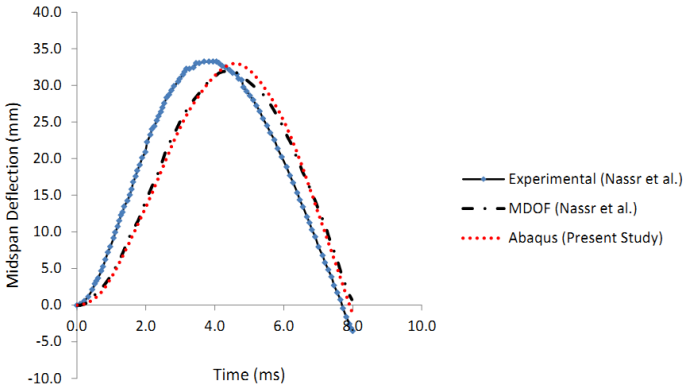

Figure 7. Mid-span deflection of B2 beam

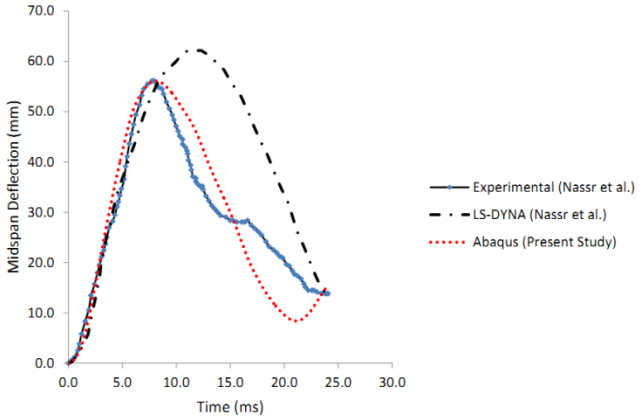

Figure 8. Mid-span deflection of C1 column

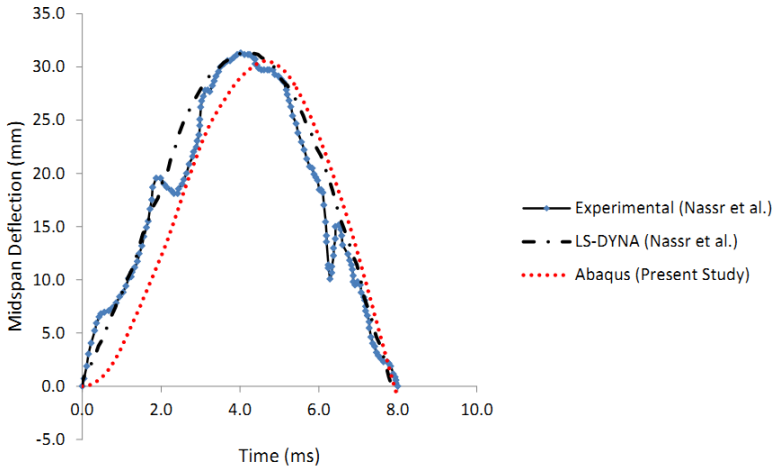

Figure 9. Mid-span deflection of C2 column

After validation the nonlinear FE model and assumptions, the structure frames are developed. For instance, Fig. 10 shows a three-story frame which is developed based on the current research assumptions using Abaqus FE software.

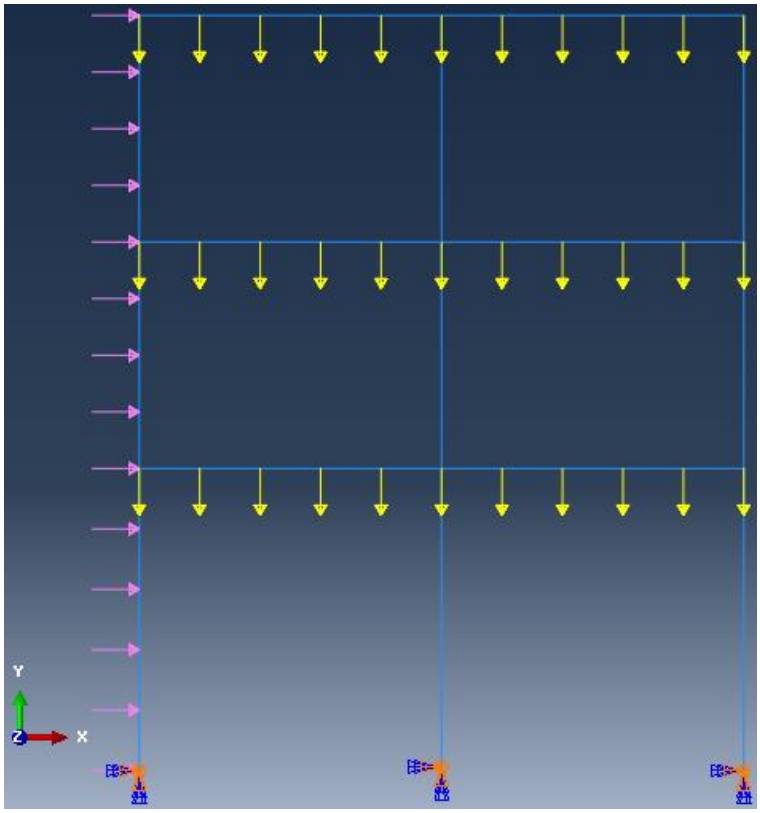

Figure 10. A three-story frame developed using Abaqus

4. OPTIMIZATION PROBLEM FORMULATION

In general, optimization is a procedure to find the best solution that it satisfies certain conditions. In multi-objective optimization the aim is to find a set of best candidate solutions called Pareto solutions or Pareto front. The general form of a multi-objective optimization problem can be written as follows:

$$min\ \{F_1(X)\ , F_2(X), \dots\dots, F_{no}(X)\} \tag{10}$$

$Subjected\ to$

$g_j(X) \leq 0 \ \ ; j = 1 \dots\dots p$

$h_k(X) = 0 \ \ ; k = 1 \dots\dots m$

$b_{li} < x_i < b_{ui}\ ;\ i = 1 \dots\dots n$

$F_1(X)$ to $F_{no}(X)$ are the objective functions, $g_j(X)$ are the inequality constraints, $h_k(X)$ are the equality constraints, x_i are the design variables, and b_{li} to $b_{ui}$are lower and upper bounds of design variables, respectively. Also, $n_o$is number of objective functions, n is number of design variables, m is number of equality constraints, and p is number of inequality constraints. In structural optimization problems, based on the problem, various objectives and constraints can be considered in the formulation. In most of the structural optimization problems, as there is a direct relationship between the structural weight and the material cost, the minimization of weight is considered as the objective function. Some other objectives which are considered in the structural problems are minimization of the structural damage, minimization of the maximum displacement, and minimization of the maximum story drifts. Also in structural problems, depending on the problem, various constraints such as stress, frequency, and deformation may be considered. Since blast loads usually are such that the structural responses may go into inelastic zone, appropriate consideration of nonlinear analysis should be taken into account. In an inelastic design it is better not to consider the strength constraints [12]. Zieman et al. [30] showed that an inelastic design could not be used to full advantage if a design was required to satisfy both strength and deformation constraints simultaneously, as the strength constraints generally prevent the structural member from yielding. Accordingly, in the present study only the deformation constraints are taken into account. According to the UFC 3-340-02 [18] criteria, design constraints are considered as story drifts and relative support rotation in beams and columns. Based on these criteria maximum allowable story drift is $H_s/25$ which H_s is the height of the $s-th$ story, and the maximum allowable relative support rotation in beams and columns for frame members is limited to 2 degrees (0.035 rad). It should be noted that based on the UFC code, the relative support rotation in members is measured as the angle between the maximum deflection point and the member's chord, as shown in Figs. 10 and 11.

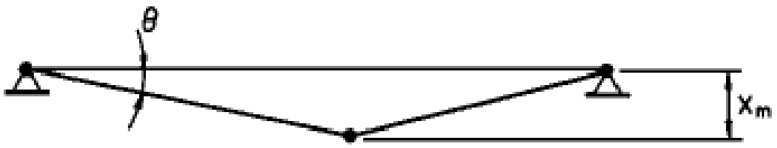

Figure 10. Relative support rotation in beam members [18]

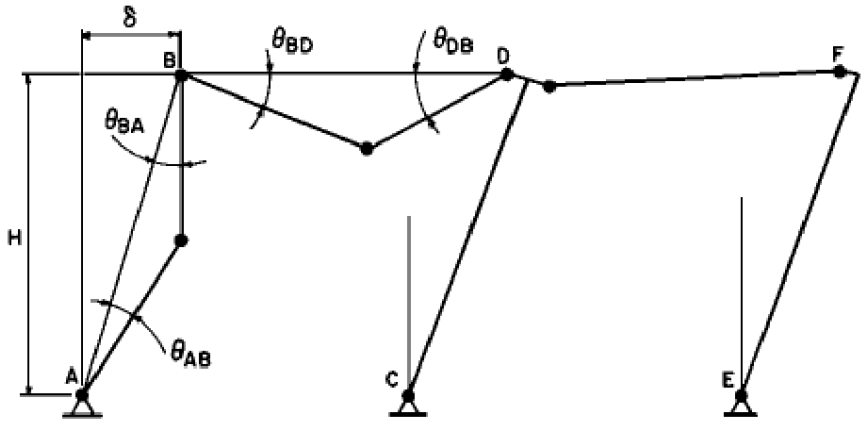

Figure 11. Relative support rotation in frame members [18]

In the present study two objectives are considered. The minimization of the structural weight to obtain low cost designs and the minimization of the inter-story drift to obtain higher performance designs. For comparison purposes and choose a better objective to represent the inter-story drifts, we have considered two cases for considering the maximum inter-story drifts. In case-I the objective is to minimize the structural weight and MaxDrift function. MaxDrift function is considered as follows:

$$MaxDrift = Max\left(\frac{drift_1}{drift_{1all}}, \frac{drift_2}{drift_{2all}}, \dots\dots, \frac{drift_{ns}}{drift_{nsall}}\right) \tag{11}$$

where, ns is the number of stories, and $drift_1 to\ drift_{ns}$ are the maximum inter-story drifts of the first story to the last one. Also, $drift_{1all}$to $drift_{nsall}$ are the allowable drift of the first story to the last story. In case-II the objective is to minimize the structural weight and AveDriftMax function. AveDriftMax is developed as follows:

$$AveDriftMax = (\frac{drift_1}{drift_{1all}} + \frac{drift_2}{drift_{2all}} + \cdots + \frac{drift_{ns}}{drift_{nsall}})/ns \tag{12}$$

On the other words:

$MaxDrift: maximum\ inter-story\ drift\ among\ all\ stories$

$AveDriftMax: average\ of\ maximum\ inter-story\ of\ all\ stories$

The considered objective functions can be summarized as follows:

$$f_1 = [\sum_{m=1}^{n_m} (\gamma L_m A_m)]/W_{max} \tag{13}$$

$$f_2 = Max\left(\frac{drift_1}{drift_{1all}}, \frac{drift_2}{drift_{2all}}, \dots\dots, \frac{drift_{ns}}{drift_{nsall}}\right) \tag{14}$$

$$f_3 = (\frac{drift_1}{drift_{1all}} + \frac{drift_2}{drift_{2all}} + \cdots + \frac{drift_{ns}}{drift_{nsall}})/ns \tag{15}$$

where, L_m is the length of the m-th member, and A_m is the cross-sectional area of the m-th member, and γ is the material specific weight that equals to 7850 (kgf/m^3), and $W_{max}$is the maximum possible weight of the structure. W_{max} can be easily calculated by considering the upper bound limits of the design variables. The above formulation is a scaled form that all objective will be in the range of $0 < f_i \leq 1$. This scaling is considered to have a better formulation. The multi-objective problem formulation is considered as follows:

$$Min \quad f \tag{16}$$

$Subject\ to$:

$$\frac{\varphi_{m,max}}{\varphi_{all}} \leq 1 \qquad (m = 1, \dots\dots\dots, n_m)$$

$$\frac{\delta_{s,max}}{\delta_{s,all}} \leq 1 \qquad (S = 1, \dots\dots\dots, n_s)$$

where, $\varphi_{m,max}$ is the maximum support rotation of $m-th$ member, φ_{all} is the allowable support rotation of members, $\delta_{s,max}$ is the maximum story drift of $s-th$ story, $\delta_{s,all}$ is the allowable drift for $s-th$ story, and n_s is the number of stories. Also additional constraints are considered as follows to ensure that the columns sections of upper stories will not be greater than the lower stories column sections:

$for\ each\ column$: $\quad A_{mi} \geq A_{mj} \quad (i < j)$

where A_{mi} is the cross-sectional area of the column m at the $i-th$ story, and A_{mj} is the cross-sectional area of the column m at the $j-th$ story.

As stated before, the objective function f is a two objective function that in the case-I we have:

$f = \{f_1 \quad f_2\}$

And in the case-II, the objective function is as follows:

$f = \{f_1 \quad f_3\}$

In the present study the multi-objective none-dominated sorting genetic algorithm (NSGA-II) is used as the optimization technique. This method is developed by Deb et al [31]. In this method each objective is treated separately and the common mutation and crossover operations are performed on the designs. The selection procedure is based on two mechanisms: “none-dominated sorting” and “crowding distance sorting”. None-dominated sorting means that the improvement in one objective is impossible without sacrificing the other objective or objectives. On the other words, design $x_1$dominates the design x_2 if two conditions are satisfied:

1- The design x_1 is not worse than the design x_2:

$f_i(x_1) \geq f_i(x_2) \quad For\ all\ i = 1,2, \dots, M$

2- The design x_1 is better than $x_2$in at least one objective:

$f_j(x_1) > f_j(x_2) \quad For\ at\ least\ one\ j \in \{1,2, \dots, M\}$

In Fig. 12 an example of dominant and none-dominant solutions is illustrated for a two objective problem. In this figure the design A dominates the design C, because it is better in both objectives. But, the designs A and B are non-dominating to each other, because each one of them is better than the other in one objective and is worse in the other objective.

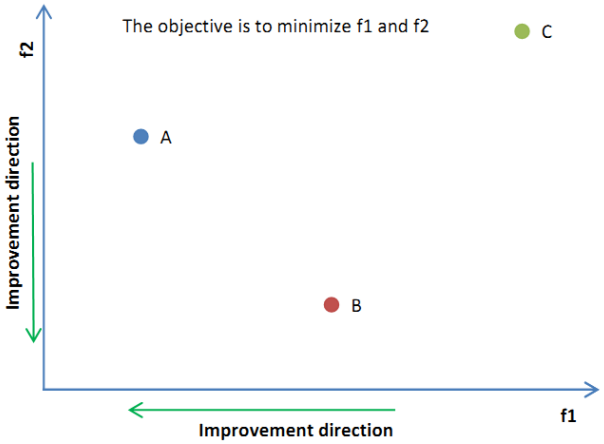

Figure 12. Dominant and non-dominant designs for a two objective optimization problem

Crowding distance is a measure of how close a design is to its neighbors. Using the crowding distance leads to better diversion of the solutions. For a two objective problem the crowding distance is shown in Fig. 13.

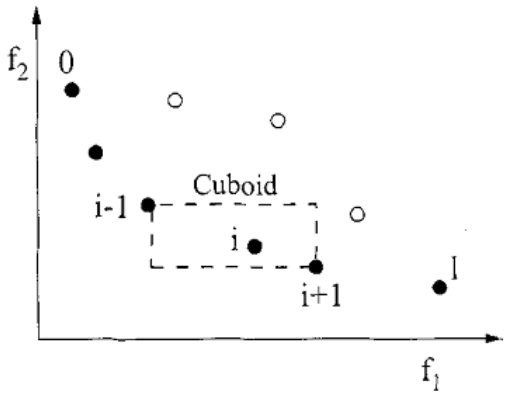

Figure 13. The crowding distance concept [31]

According to Fig. 13, the crowding distance for a two-objective optimization is calculated as follows:

$$d_i^1 = \frac{\left|f_1^{i+1} - f_1^{i-1}\right|}{f_1^{max} - f_1^{min}} \tag{17}$$

$$d_i^2 = \frac{\left|f_2^{i+1} - f_2^{i-1}\right|}{f_2^{max} - f_2^{min}} \tag{18}$$

$$d_i = d_i^1 + d_i^2 \tag{19}$$

In each iteration of the NSGA II method, a Pareto set is constructed so that each design has the best combination of objective functions and improvement in an objective is

impossible without sacrificing other objectives.

Here, a design methodology is proposed for the considered multi-objective optimization problem. The flowchart of this method is shown in Fig. 14. According to the proposed method, first the finite element model is created and initialized. This includes applying gravitational and blast loads on the structure and initializing the design variables. In the present research, the cross-sectional areas of members are considered as the design variables. The other geometrical properties of the sections such as section depth, width, flange and web thicknesses are computed based on some equations of cross-sectional areas. These equations can be easily derived by performing regression analysis on available steel profile sections such as AISC or DIN 1025 I-shape sections. The design space can be considered as continuous or discrete space. In the next step the nonlinear explicit dynamic finite element analysis is performed. Unlike seismic structural analysis problems, the explicit nonlinear dynamic analysis is very computationally inexpensive in the blast analysis problems. Furthermore, using this type of structural analysis, results in relatively accurate and realistic results. By performing the nonlinear structural analysis, the nonlinear responses are derived. These responses include the maximum inter-story drifts, and the maximum relative support rotation in beams and columns. Then, based on the optimization problem formulation, an optimization step is performed using NSGA-II method. These steps are repeated until the stopping criteria are satisfied. Based on the proposed methodology a framework is developed and two numerical examples are studied which are presented in the next section.

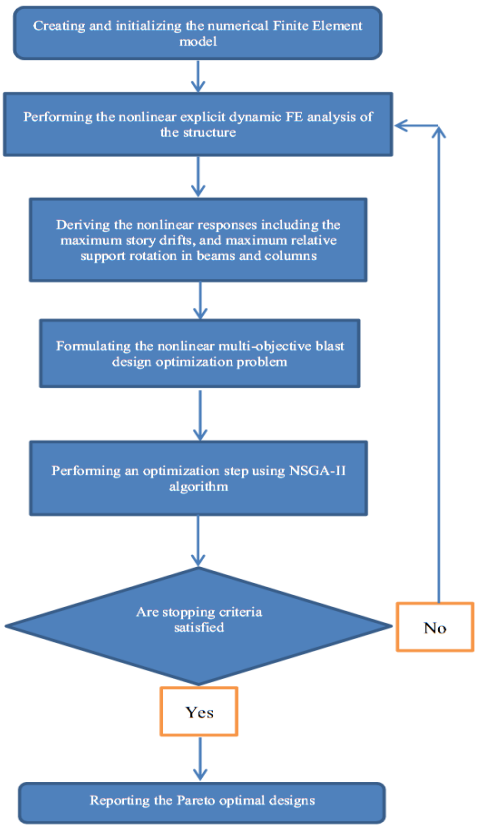

Figure 14. Flowchart of the proposed method

5. NUMERICAL EXAMPLES

The following assumptions are made throughout the studied examples:

Three types of loading are considered which are dead, live and blast loads. In all stories dead and live loads are assumed to be $6kN/m^2$ and $2kN/m^2$, respectively. The tributary widths of the studied frames are assumed to be 4 m. It is assumed that based on the blast threat analysis, the structure is designed for a surface blast of 150 kg TNT equivalent and a standoff distance of 15 m. As the scaled blast distance is $2.82 > 1.2\ m/kg^{1/3}$, the explosion is classified as far-range blast. Thus, the blast loading profile has been assumed as a uniform time-history loading acting on the front side of the structure. Also, as suggested in "Handbook for Blast-Resistant Design of Buildings" [32], the load combination is considered as follows:

$$1.0\ DL+0.25\ LL+1.0\ B \tag{20}$$

where DL is the dead load, LL is the live load, and B is the blast load acting on the structure. Design constraints are considered based on UFC 3-340-02 [18] criteria. These constraints are the maximum story drift and relative support rotation in beams and columns. Based on the UFC criteria, allowable drift is limited to H/25, and the allowable relative support rotation is limited to 2 degrees (0.035 rad). The objectives of the problem are minimizing the structural weight and minimizing the maximum inter-story drift. For all members Yield stress is $240Mpa$, and Young's modulus is $2e5Mpa$. Design variables are the cross-sectional areas of members. Other geometrical properties of frame member sections have been formulated based on the European DIN 1025 standard profiles, as functions of the cross-sectional areas. IPB (HEB) profiles are used for columns, and IPE profiles are used for beam members. Design variables are assumed as discrete variables in the design space. Lower bound limit of the columns cross-sectional areas is set to 4300 mm^2 corresponding to IPB 14 and the upper bound is limited to 19800 mm^2 corresponding to IPB 40. Similarly, the Lower bound of the beams cross-sectional areas is limited to 2010 mm^2 corresponding to IPE 16 and the upper bound is limited to 8450 mm^2 corresponding to IPE 40. In the studied examples the objective function is considered in two separate cases. In case I the objective is to minimize the structural weight and the MaxDrift function, and in case II the objective is to minimize the structural weight and the AveDriftMax function. All the examples are solved by parallel processing using a laptop computer with Intel Core i7 processor and 8GB RAM.

5.1 Three-story two-bay example

A three-story steel moment resisting steel frame is considered in this numerical example. The frame topology is shown in Fig. 15. Six section groups are considered as shown in Fig. 15 by numbers 1 to 6. According to the proposed method the optimization process has been performed. In addition of structural weight, the two other objectives (MaxDrift and AveDriftMax) are considered separately as the second objectives. The obtained optimal Pareto fronts are shown in Figs. 16 and 17. For this example the size of population and number of generations were set to 12 and 70, respectively. The execution time for

performing the optimization of this example in Case-I was 1 hour and 45 minutes, and in Case-II it was 1 hour and 52 minutes.

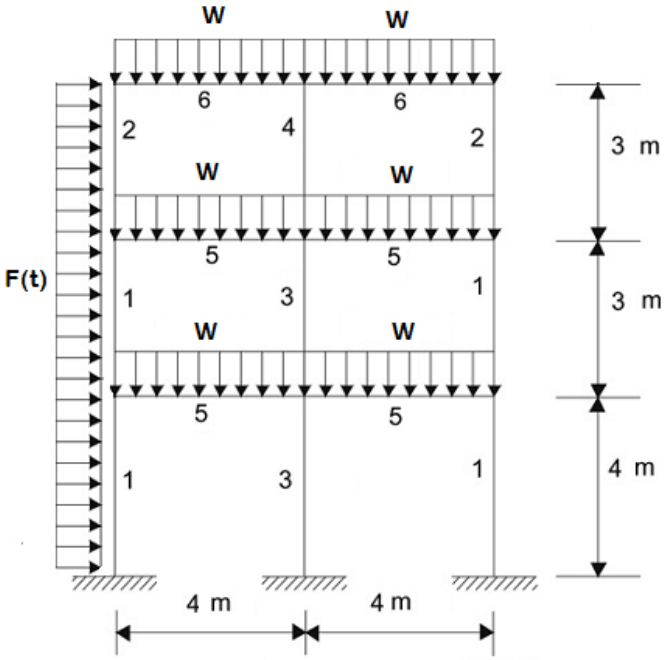

Figure 15. Topology of the six story frame

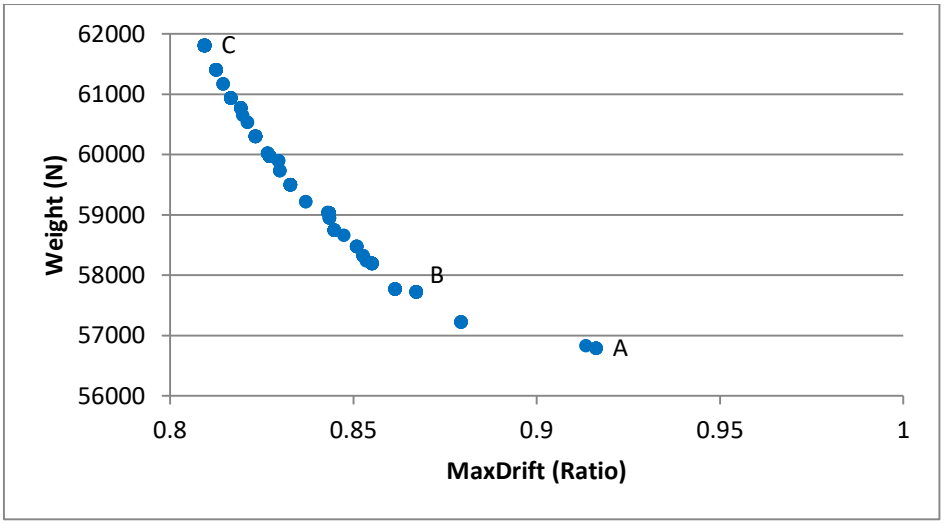

Figure 16. Obtained optimal Pareto solutions for the three-story example by using MaxDrift objective

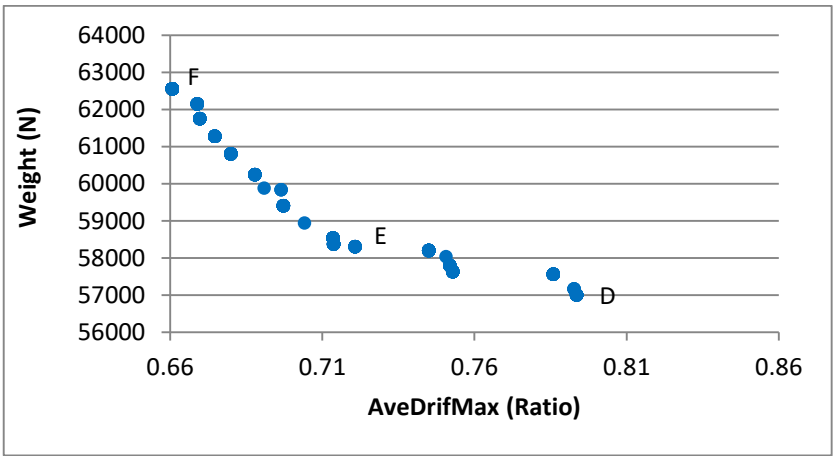

Figure 17. Obtained optimal Pareto solutions for the three-story example by using AveDriftMax objective

We consider three designs from each of the Pareto frontiers for reviewing the drift results. These designs are shown in Figs. 16 and 17 as A, B, C, D, E, and F. Design A, B, and C are obtained in case-I and designs D, E, and F are obtained in case-II. In case-I, design A is a design with lowest weight, design C is a design with lowest MaxDrift ratio, and design B is a design with a maximum inter-story approximately average of A and C ($MaxDrift_B\ Ratio = 0.867$). Similarly, in case-II, design D is a design with lowest weight, design F is a design with lowest AveDriftMax ratio, and design E is a design with a maximum inter-story approximately average of D and F ($AveMaxDrift_E\ Ratio = 0.72$). Properties of the selected designs are summarized in Table 3.

Table 3: Properties of the selected optimal designs in the first example

	Design A	Design B	Design C	Design D	Design E	Design F
$Section\ Group\ 1$	IPB 40	IPB 40	IPB 40	IPB 36	IPB 36	IPB 40
$Section\ Group\ 2$	IPB 32	IPB 32	IPB 40	IPB 30	IPB 32	IPB 40
$Section\ Group\ 3$	IPB 36	IPB 40	IPB 40	IPB 40	IPB 40	IPB 40
$Section\ Group\ 4$	IPB 30	IPB 30	IPB 40	IPB 40	IPB 34	IPB 40
$Section\ Group\ 5$	IPE 40	IPE 40	IPE 40	IPE 40	IPE 40	IPE 40
$Section\ Group\ 6$	IPE 30	IPE 30	IPE 36	IPE 33	IPE 40	IPE 40
$MaxDrift\ (Ratio)$	0.92	0.867	0.81	1	1	0.72
$AveMaxDrift\ (Ratio)$	0.7	0.82	0.7	0.793	0.72	0.66
$Weight\ (N)$	56790	57724	61808	56997	58302	62549

The maximum inter-story drifts for the selected designs are plotted in Fig. 18. Form this figure it can be concluded that in the case-I, the drift distributions among the stories are more uniform, comparing to the case-II. In designs D and E, the maximum inter-story of the first story is higher than the other designs, but their maximum inter-story drifts of the other stories are low. The design A has the lowest weight among the all selected optimal designs, but according to Fig. 18 its maximum inter-story drift is not the highest one among the selected designs. Also, among the all designs, the design B is the design with most uniform

drift distribution. Both Designs A and B are obtained in case-I. The design E and F have the lowest maximum drift among the selected designs. Design F has the maximum weight among the selected designs. Both designs E and F are obtained in case II.

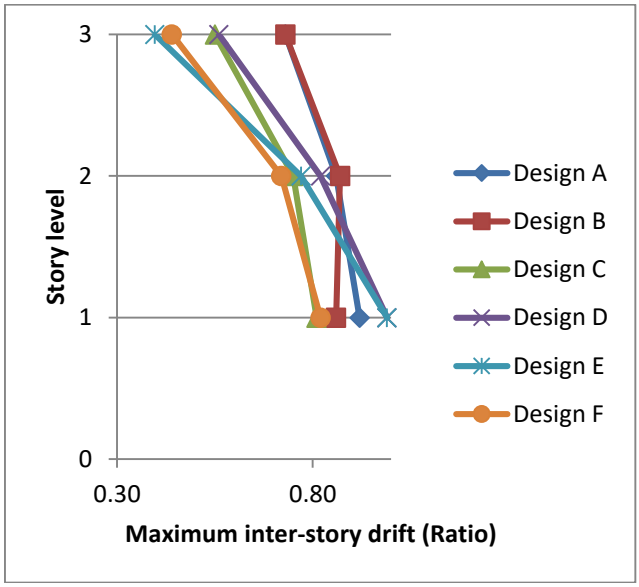

Figure 18. maximum inter-story drifts of the selected optimal designs in the first example

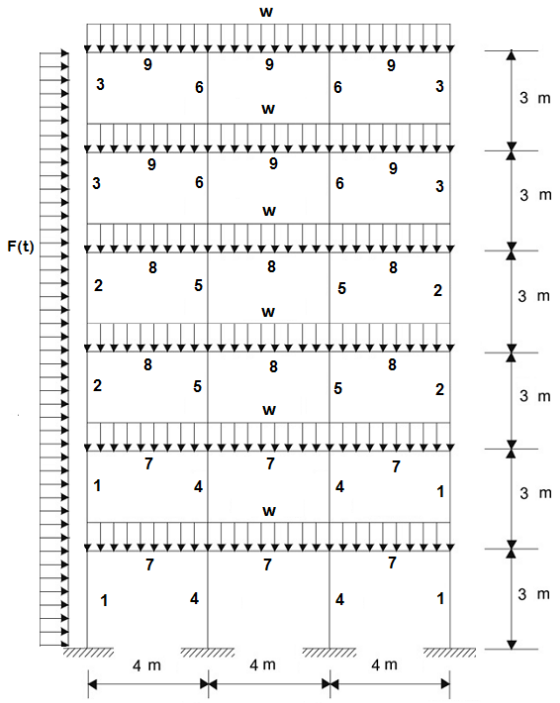

Figure 19. Topology of the six story frame

5.2 Six-story three-bay example

A six-story steel moment resisting steel frame is considered in this example. The frame topology is shown in Fig. 19. Nine section groups are considered as shown in Fig. 19 by numbers 1 to 9. According to the proposed method the optimization process has been performed. In addition of structural weight, the two other objectives (MaxDrift and AveDriftMax) are considered separately as the second objectives. The obtained optimal Pareto fronts are shown in Figs. 20 and 21. For this example the size of population and number of generations were set to 20 and 180, respectively. The execution time for performing the optimization of this example in Case-I was 10 hours and 1 minute, and in Case-II it was 9 hours and 50 minutes.

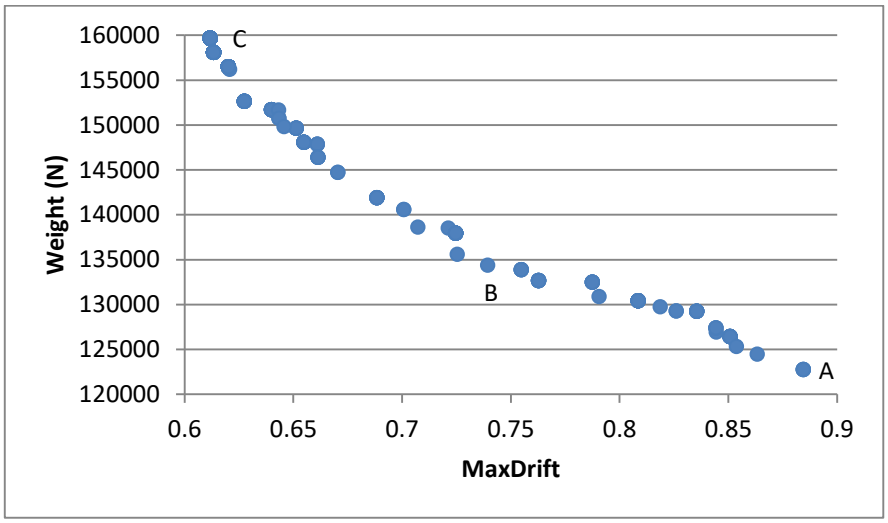

Figure 20. Obtained optimal Pareto solutions for the six-story example by using MaxDrift objective

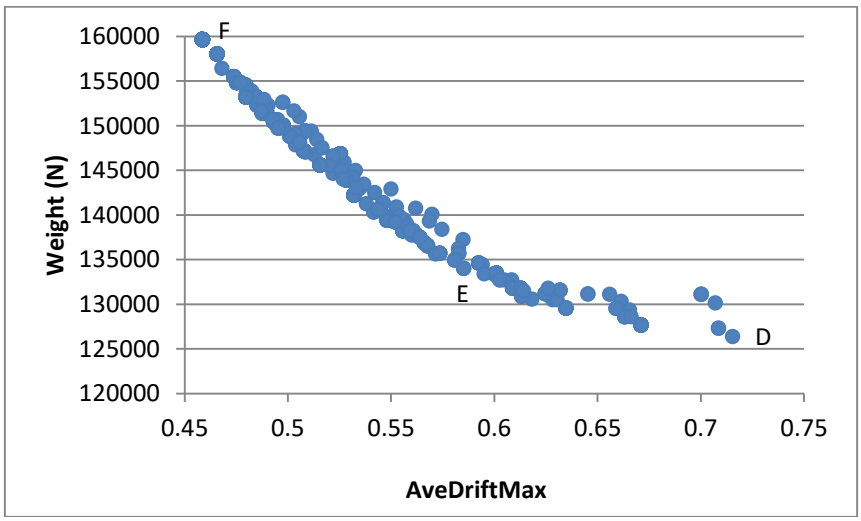

Figure 21. Obtained optimal Pareto solutions for the six-story example by using AveDriftMax objective

We consider three designs from each of the Pareto frontiers for reviewing the drift results. These designs are shown in Fig. 20 and 21 as A, B, C, D, E, and F. Designs A, B, and C, are obtained in Case-I, and designs D, E, F, are obtained in case-II. In case-I, design A is a design with lowest weight, design C is a design with lowest MaxDrift ratio, and design B is a design with a maximum inter-story approximately average of A and C ($MaxDrift_B\ Ratio = 0.739$). Similarly, in case-II, design D is a design with lowest weight, design F is a design with lowest AveDriftMax ratio, and design E is a design with a maximum inter-story approximately average of D and F ($AveMaxDrift_E\ Ratio = 0.585$). Properties of the selected designs are summarized in Table 4.

Table 4: properties of the selected optimal designs in the second example

	Design A	Design B	Design C	Design D	Design E	Design F
$Section\ Group\ 1$	IPB 30	IPB 30	IPB 40	IPB 34	IPB 34	IPB 40
$Section\ Group\ 2$	IPB 30	IPB 30	IPB 40	IPB 28	IPB 28	IPB 40
$Section\ Group\ 3$	IPB 28	IPB 28	IPB 40	IPB 28	IPB 28	IPB 40
$Section\ Group\ 4$	IPB 34	IPB 40	IPB 40	IPB 36	IPB 36	IPB 40
$Section\ Group\ 5$	IPB 30	IPB 40	IPB 40	IPB 36	IPB 34	IPB 40
$Section\ Group\ 6$	IPB 22	IPB 28	IPB 40	IPB 28	IPB 28	IPB 40
$Section\ Group\ 7$	IPE 40	IPE 40	IPE 40	IPE 36	IPE 40	IPE 40
$Section\ Group\ 8$	IPE 40	IPE 40	IPE 40	IPE 36	IPE 40	IPE 40
$Section\ Group\ 9$	IPE 40	IPE 36	IPE 40	IPE 33	IPE 40	IPE 40
$MaxDrift\ (Ratio)$	0.88	0.74	0.61	0.997	0.81	0.61
$AveMaxDrift\ (Ratio)$	0.7	0.6	0.46	0.72	0.585	0.46
$Weight\ (N)$	122761	134367	159669	126416	134046	159669

The maximum inter-story drifts for the selected designs are plotted in Fig. 22. Form this figure it can be seen that in the case-I, the drift distributions among the stories are more uniform, comparing to the case-II. The design A has the lowest weight among the selected designs, but its maximum drift is not the highest drift among the selected designs. According to Fig. 22 the designs C and F have the lowest maximum drift among the all selected designs. Designs A and C are obtained in case I. Also, the design F belongs to case II. It should be noted that the designs C and F have equal properties and all members sections in these two designs are the upper-bound limits of the sections. Among all the designs, design B has the most uniform distribution of drifts between the stories. Also by comparing the design B and E, it is evident that the structural weights of these two designs are approximately the same. But the maximum inter-story drift of design B is lower than design C. Also, according to Fig. 22, the drift distribution of design B is more uniform than design E. Design B is obtained in case-I and design E is obtained in case-II.

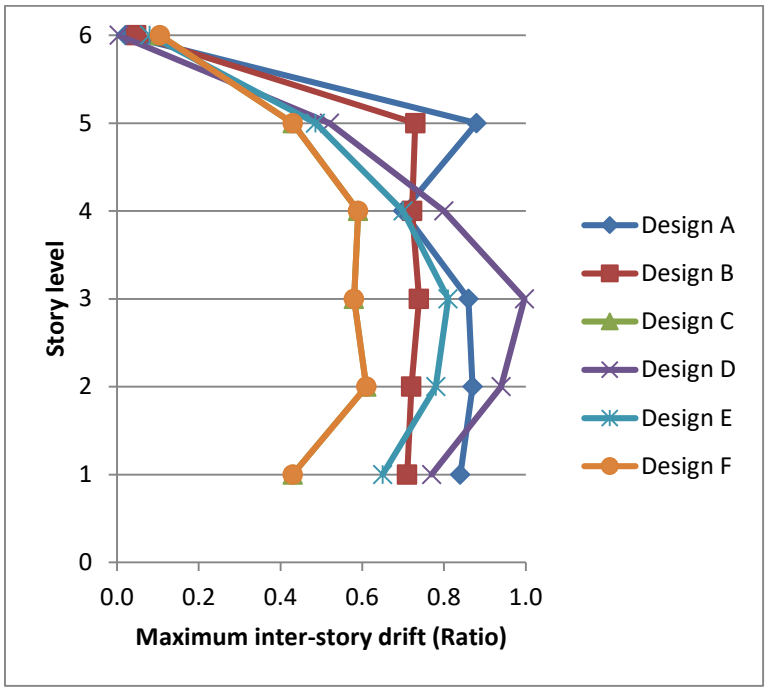

Figure 22. maximum inter-story drifts of the selected optimal designs in the second example

6. SUMMARY AND CONCLUSIONS

In the present paper, a multi-objective optimization of steel moment frames against blast loading was studied. For this purpose first an optimization methodology was proposed for the problem. The proposed method is constructed by combining the nonlinear explicit dynamic finite element analysis of the structure and the NSGA II optimization algorithm. Unlike the seismic problems, the nonlinear explicit dynamic analysis is very computationally inexpensive in the blast analysis problems. This advantage makes the proposed method practical and relatively computationally inexpensive. The considered objectives were minimization of the structural weight and minimization of the maximum inter-story drifts. In the structural problems, lower drift designs are related to have higher performance designs. Thus, minimization of the drifts was considered to obtain higher performance designs. The maximum inter-story drifts were considered in two separate cases to compare the results. In the first case the drift-related objective was the minimization of the maximum inter-story drift among all the stories. In the second case the drift-related objective was minimization of the average of maximum inter-story drifts of all stories. Two numerical examples were considered. In the studied examples it was observed that in the case-I the distribution of maximum drifts were more uniform than in the case-II. Also, the obtained lowest weight design in case-I was lighter than the obtained lowest weight design of case-II. From the results of the numerical examples it can be concluded that the case-I had better results than case-II. This study shows that in the problem of optimum blast design of steel moment frames, the considered methodology, especially in case-I, is very effective and practical and can be used to obtain practical low-cost and high-performance designs. Also,

according to the owner's budget, designs with desired performance levels can be chosen from the obtained Pareto solutions.

REFERENCES

1. Taylor GI. Notes on the Dynamics of Shock Waves from Bar Explosive Charges, UK Ministry of Home Security, Civil Defense Research Committee Paper, 1940.
2. Taylor GI. The Propagation and Decay of Blast Waves, UK Home Office, ARP department, 1941.
3. Taylor GI. The Propagation of Blast Waves over the Ground, UK Ministry of Home Security, Civil Defense Research Committee paper, 1941.
4. Hadianfard MA, Farahani A, B-Jahromi A. On the effect of steel columns cross sectional properties on the behaviours when subjected to blast loading, *Struct Eng Mech* 2012;**44**(4).
5. Nassr AA, Razaqpur AG, Tait MJ, Campidelli M, Foo S. Single and multi-degree of freedom analysis of steel beams under blast loading, *Nucl Eng Des* 2012; **242**: 63-77.
6. Monir HS. Flexible blast resistant steel structures by using unidirectional passive dampers, *J Constr Steel Res* 2013; **90**: 98-107.
7. Nassr AA, Razaqpur AG, Tait MJ, Campidelli M, Foo S. Dynamic response of steel columns subjected to blast loading, *J Struct Eng (ASCE)* 2014; **140**(7): 600-619.
8. Coffield A, Adeli H. An investigation of the effectiveness of the framing systems in steel structures subjected to blast loading, *J Civil Eng Manag* 2014, **20**(6): 767-77.
9. Elsanadedy HM, Almusallam TH, Alharbi YR, Al-Salloum YA, Abbas H. Progressive collapse potential of a typical steel building due to blast attacks, *J Constr Steel Res* 2014; **101**: 143-57.
10. Lee K, Shin J. Equivalent single-degree-of-freedom analysis for blast-resistant design, *Int J Steel Struct* 2016; **16**(4): 1263-71.
11. Kaveh A, Laknejadi K, Alinejad B. Performance-based multi-objective optimization of large steel structures, *Acta Mech* 2012; **223**(2): 355-69.
12. Gong Y, Xue Y, Xu L, Grierson DE. Energy-based design optimization of steel building frameworks using nonlinear response history analysis, *J Constr Steel Res* 2012; **68**(1): 43-50.
13. Kaveh A, Fahimi-Farzam M, Kalateh-Ahani M. Optimum design of steel frame structures considering construction cost and seismic damage, *Smart Struct Syst* 2015; **16**(1): 1-26.
14. Gholizadeh S, Baghchevan A. Multi-objective seismic design optimization of steel frames by a chaotic meta-heuristic algorithm, *Eng Comput* 2017; **33**(4): 1045-60.
15. Babaei M, Sanaei E. Multi-objective optimal design of braced frames using hybrid genetic and ant colony optimization, *Front Struct Civ Eng* 2016; **10**(4): 472-80.
16. Barraza M, Bojórquez E, Fernández-González E, Reyes-Salazar A. Multi-objective optimization of structural steel buildings under earthquake loads using NSGA-II and PSO, *KSCE J Civ Eng* 2017; **21**(2): 488-500.

17. Rezazadeh F, Mirghaderi R, Hosseini A, Talatahari S. Optimum energy-based design of BRB frames using nonlinear response history analysis, *Struct Multidiscip Optim* 2017: 1-15.
18. US Department of Defense. UFC 3-340-02: Structures to Resist the Effects of Accidental Explosions, 2008.
19. Cormie D, Mays G, Smith P. *Blast Effects on Buildings* (Second Edition), Thomas Telford Publishing, London, UK, 2009.
20. American Society of Civil Engineers. *Blast Protection of Buildings*, American Society of Civil Engineers/Structural Engineering Institute, 2011.
21. Miyamoto HK, Taylor D. Structural control of dynamic blast loading, In: *ASCE Conference American Society of Civil Engineers* 2004, pp. 1-8.
22. Motley MR, Plaut RH. Application of synthetic fiber ropes to reduce blast response of a portal frame, *Int J Struct Stab Dyn* 2006; **6**(4): 513-26.
23. Löfquist C. Response of Buildings Exposed to Blast Load Method Evaluation, MSc Thesis, Lund University, 2016.
24. FEMA. *Risk Assessment - A How-To Guide to Mitigate Potential Terrorist Attacks Against Buildings*, A how-to Guid to mitigate potential Terror attacks against Build, 2005; January, pp. 1-248.
25. Abaqus, V. 6.10 Documentation. Dassault Systemes Simulia Corporation, 2010.
26. Borst R de, Crisfield MA, Remmers JJC, Verhoosel C V. *Non-Linear Finite Element Analysis of Solids and Structures*, 2nd Ed, 2012; **25**.
27. Nassr AA. Experimental and Analytical Study of the Dynamic Response of Steel Beams and Columns To Blast. PhD Thesis, McMaster University, 2012.
28. Ziemian RD, McGuire W, Deierlein GG. Inelastic Limit States Design. Part I: Planar Frame Studies, *J Struct Eng, ASCE* 1992; **118**(9): 2532.
29. Deb K, Pratap A, Agarwal S, Meyarivan T. A fast and elitist multi-objective genetic algorithm: NSGA-II, *IEEE Trans Evol Comput* 2002; **6**(2): 182-97.
30. Dusenberry DO. *Handbook for Blast Resistant Design of Buildings*, John Wiley & Sons, New Jersey, 2010.